

## HYPERSPECTRAL IMAGING OF MARTIAN AND LUNAR METEORITES BY SCANNING LABORATORY SOURCE X-RAY MICROFLUORESCENCE SPECTROMETRY: A NEW TOOL FOR PLANETARY SCIENCE.

E. P. Vicenzi<sup>1,2</sup>, J. Davis<sup>2</sup>, P. K. Carpenter<sup>3</sup>, R. A. Zeigler<sup>3</sup>, and B. L. Jolliff<sup>3</sup>.  
<sup>1</sup>Department of Mineral Sciences, Smithsonian Institution, Washington, DC; <sup>2</sup>Surface and Microanalysis Science Division, NIST, Gaithersburg, MD; <sup>3</sup>Department of Earth and Planetary Sciences, Washington University, St. Louis, MO. (vicenzie@si.edu)

**Introduction:** The field of microanalysis has seen significant advancements in recent years with the concurrent development of particle/photon beam microscopes and increasingly sophisticated detection schemes for secondary signals (e.g. X-rays, electrons, UV-VIS-NIR). While many of these advancements have been made in pushing the limits of high spatial resolution analysis of extraterrestrial materials, few techniques allow one to readily and efficiently probe the elemental composition of samples between the micrometer and centimeter length scales. Laboratory source scanning X-ray microfluorescence spectrometry ( $\mu$ XRF) fills such an analytical gap with an excitation volume of roughly 100  $\mu$ m/pixel for polished thick specimens. Despite the obvious limitations of the inability to spatially resolve fine-scale phases, hyperspectral  $\mu$ XRF, allows for rapid estimation of the chemistry of the entire area exposed in a conventionally-mounted rock section. Similarly, it is desirable in some studies to discern sub-sample volumes defined by lithological (or other) boundaries and compute their "bulk" chemistry, a problem ideally suited for hyperspectral  $\mu$ XRF.

**Analytical methods:** *Data collection.* X-ray fluorescence data were collected using an EDAX Eagle III using the procedures defined by Davis et al [1]. Primary Rh X-rays generated by 40 keV electrons, oriented orthogonal to the sample, were used to produce secondary fluorescence in several meteoritic specimens. A capillary optic was employed to reduce the primary X-ray spot size to roughly 40  $\mu$ m in diameter. A conventional Si(Li) X-ray detector and digital pulse processor were used along with a pulse processing time constant of 6.4  $\mu$ sec to store ~15,000 counts per second. Specimens were rastered to sequentially compile a 3 D hyperspectral X-ray data cube. Each spectrum contains X-ray data from <1 to 25 keV at 2 bytes depth. Pixel dwell times for X-ray collection ranged from 5-30 seconds in duration.

*Data processing.* Image processing was performed on two platforms. Using EDAX Vision 32 software, a series of quantified energy region of interest maps were generated from the data cube where gray scale values represent weight percent of the oxide for the various metals. This software employs a fundamental

parameters method of quantification with the addition of empirical standards, similar to the method developed by Criss et. al. [2]. Additional image processing and data extractions were performed by Lispix [3], including the production of the maximum pixel spectrum to reveal low probability X-ray occurrences [4].

**Results:** *Martian meteorite NWA 817.* The large dynamic range of  $\mu$ XRF enables the simultaneous collection of major, minor, and trace element images (Figure 1). High intensity regions of the Ca, Fe, and K images reveal Ca-pyroxene, olivine, and the mesostasis, the 3 major phases of the meteorite. Minor element imaging highlighted a second pyroxene enriched in Mn as well as rutile and a phosphate. Trace Sr is enriched in feldspars within former melt pockets. Initial attempts to quantify spectra indicate Sr is present at the hundreds of ppm concentration level in mesostasis feldspar. Because the entire X-ray data cube is available for post processing, multivariate statistical analysis can also be performed. In Figure 2 we show the composite of the 1<sup>st</sup>, 2<sup>nd</sup>, and 3<sup>rd</sup> principal component score images that indicate all major phases plus the Mn-rich pyroxene. Because phase spectra can be extracted by summing each pixel in each phase, the bulk chemistry can therefore be computed.

*Lunar meteorite Dhofar 961.* Dhofar 961 is a mafic lunar meteorite with impact-melt lithic clasts characterized by variations in bulk chemistry and fine-scale textural variation, and is described by Jolliff et al. [5]. Compositional mapping using the electron microprobe, coupled with spot microanalysis of mineral phases and broad-beam analysis of ~50  $\mu$ m regions, enables the calculation of bulk composition via modal analysis. Raw intensity and quantitative XRF maps supplement the microprobe data and provide additional discrimination between and within the lithic clasts (Figure 3). Specifically, the Mg, Al, and Fe data delineate internal structure that is not apparent on the BSE image. The calculation of local bulk composition via XRF data is less complicated than for EPMA and provides superior detection of minor and trace elements. Conversely, the ~ 100  $\mu$ m interaction volume results in averaging of x-rays from multiple phases during data collection, which must be deconvolved to end member components during analysis.

**References:**

[1] Davis J. et al. (in review) *J. Amer. Ceramic Soc.* [2] Criss J.W. et al. (1978) *Analytical Chemistry* 50: 33-37. [3] Bright D.B. (2000) *Scanning* 22: 111-112. [4] Bright D.B. and Newbury D.E. (2004) *J. Microscopy* 216: 186-193. [5] Jolliff B. L. et al. (2008) *LPS XXXIX, this volume.*

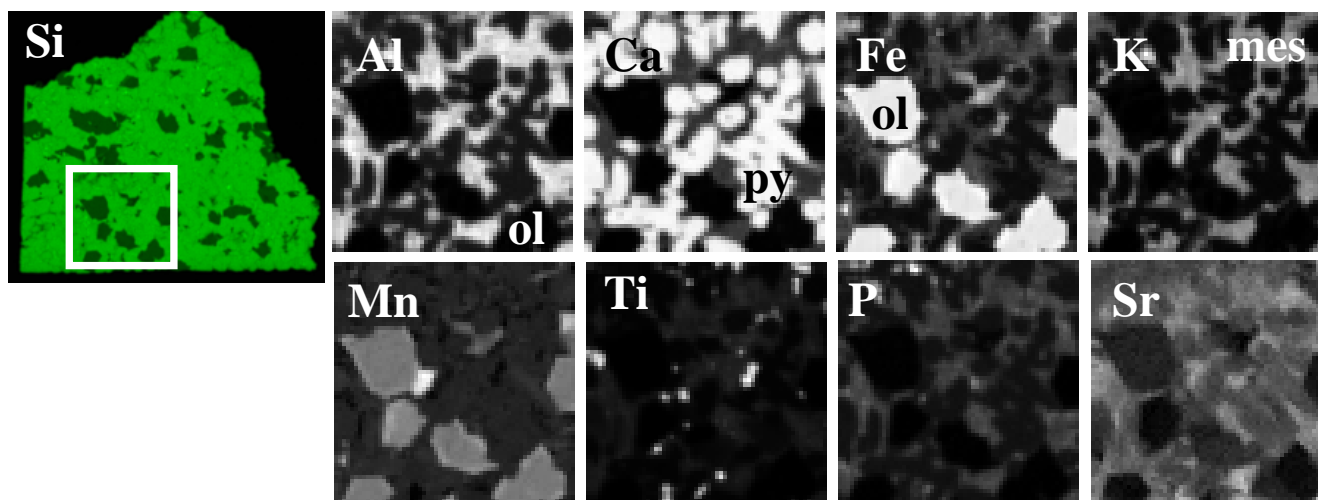


Figure 1. Si overview image of Martian nakhlite NWA 817 (HFW=10.5 mm) with 3 x 3 mm rectangle showing area of longer duration imaging. The high dynamic range of  $\mu$ XRF allows for simultaneous collection of major element (Al, Ca, Fe, and K), minor element (Mn, Ti, and P), and trace element (Sr) images.

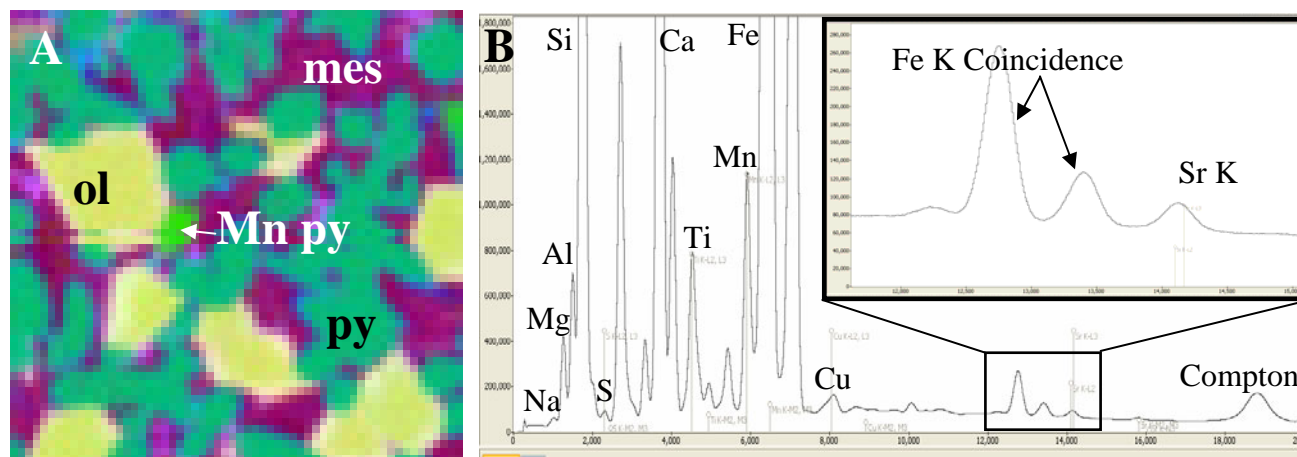


Figure 2. A) An RGB composite image of the 1<sup>st</sup>, 2<sup>nd</sup>, and 3<sup>rd</sup> principal component score images derived from the hyperspectral X-ray data cube highlighting the major phases present in NWA 817, including: olivine (yellow), Ca-pyroxene (green), mesostasis (maroon/magenta), and a Mn-rich Ca pyroxene (bright green). B) Integrated or sum spectrum for entire image including X-ray artifacts (Fe coincidence peaks) and trace Sr in inset.

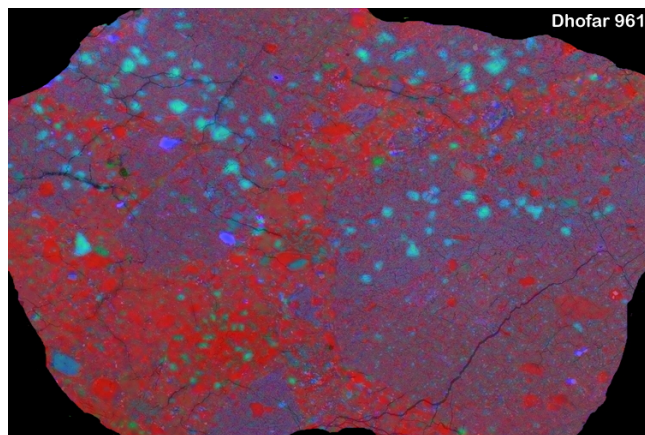


Figure 3. Composite RGB x-ray map of Dhofar 961, with Al in red, Mg in green, Fe in blue, and BSE in grayscale. The horizontal field width is 12 mm. Olivine is cyan, Mg-pyroxene blue-green, plagioclase is red. Note clear discrimination of matrix from clasts and division between upper and lower material in large clast at far right.